

Supporting Information for

Copper regulates the host innate immune response against bacterial infection via activation of ALPK1 kinase

This PDF file includes:

Supporting text (Additional Materials and Methods)
Figures S1 to S20
SI References

Supporting Information Text (Additional Materials and methods)

Zebrafish Infection model. All of the adult zebrafish including wild-type AB and Tg(*coro1a*:eGFP) zebrafish lines were obtained from Zebrafish International Resource Center(ZIRC) and were raised under standard conditions (28.5 °C, 14 hrs light/10 hrs dark). All fish were fed with hatched fairy shrimps three times each day. Male and female zebrafish were kept separately until mating and spawning. Eggs were kept in E3 medium (5 mM NaCl, 0.17 mM KCl, 0.33 mM CaCl₂, 0.33 mM MgSO₄) with 0.003% PTU to reduce melanin deposition and staged as hour post-fertilization (hpf) and day post-fertilization (dpf)

For *S. enterica* infection, zebrafish larvae were pre-treated with/without CuSO₄ (0, 4, 10 μM) in sterilized E3 embryos medium. Zebrafish was challenged with *S. enterica* (MOI 100) by immersion and sacrificed at 3~6 hpi (hours post infection). Colonization of *S. enterica* inside zebrafish was assessing by counting the colony-forming units (CFUs). All animal care and experimental protocols were approved by the Ethics Committee for Animal Experimentation at the Fifth Affiliated Hospital, Sun Yat-Sen University.

The *alpk1* knockout F0 zebrafish was established similarly as described previously (1), recombination Cas9 protein (Invitrogen), synthesized tracerRNA and five crRNAs (IGE Biotech), targeting 5 loci in *alpk1* gene, were mixed for gRNA/Cas9 complex assembly. Approximately 1 nL of gRNA/Cas9 complex (28.5 fmol [4700 pg] of Cas9 and 28.5 fmol [1000 pg] of total gRNA) was injected into the yolk at the single-cell stage before cell inflation. Headloop PCR is used to validate *alpk1* knockout in zebrafish. The headloop score (HL score) for *alpk1* was calculated as the ratio between the headloop PCR band intensity (HL) and the standard PCR band intensity (std).

Sequences for gRNAs targeting *alpk1* are listed as below.

RNA name	sequences
Universal tracrRNA	UAGCAAGUUA AAAUAAGGCUAGUCCGUUAUCAACU UGAAAAAGUGGCACCGAGUCGGUGCUUUU
crRNA-<i>alpk1</i>-A	UACCUJGCUCAAUACUCAUGCGUUUUAGAGCUA
crRNA-<i>alpk1</i>-B	AGGACGCGGCUGACAGAAAGGUUUUAGAGCUA
crRNA-<i>alpk1</i>-C	CUUCCUCAGAGACUGUAUCGGUUUUAGAGCUA
crRNA-<i>alpk1</i>-D	GAAGUCUCGCUCAUUCAUGGGUUUUAGAGCUA
crRNA-<i>alpk1</i>-E	ACAUCUUCUACUCAACCGAGGUUUUAGAGCUA

Neutrophils recruitment assay (Zebrafish model). At 4hpf, Tg(*coro1a*:eGFP) zebrafish larvae were pre-treated with CuSO₄ (4 μM) in sterilized E3 embryos medium with 0.003% PTU. At 3 dpf, zebrafish larvae were anesthetized with 0.1mg/ml tricaine and transection of the tailfin tip was performed with sterile scalpel. Zebrafish with injured tails were challenged immediately with bacterial pathogen *V. vulnificus* (MOI 100). The numbers of Neutrophils around the wound area were accessed at 0, 2, 4, and 6 hpi.

Recombination protein purification. ALPK1 recombination proteins (solo NTD or NTD-CKD complex) were overexpressed and purified similarly as described previously (2). Protein expression was induced by the addition of 0.5 mM isopropyl β -d-1-thiogalactopyranoside (IPTG) at 20 °C overnight (~16 h) after OD600 of the bacterial culture reached ca. 0.8.

To obtain solo NTD domain, pGEX-6p-2-ALPK1(1-473) vector was used. To obtain the NTD-CKD complex, pGEX-6p-2-ALPK1(1-473) and pACYC-sumo-ALPK1(959-1244) vectors were co-transformed in to *E. coli* BL21(DE3). GST-NTD or GST-NTD-CKD were purified by glutathione Sepharose affinity column. GST-tag was removed from NTD by digestion with HRV 3C protease at 4°C and SUMO-tag was removed from CKD by digestion with the home-made ULP1 protease. NTD and NTD-CKD proteins were further purified with an additional Superdex G200 gel filtration column (GE Healthcare).

To obtain full-length ALPK1, pCS-ALPK1-flag or pCS-ALPK1-His vector was transfected into HEK293t cells and culture for 48 hrs. ALPK1-flag or ALPK1-His was purified using ANTI-FLAG M2 Affinity Gel (Sigma-Aldrich) or Ni-NTA agarose resin (ThermoFisher).

To obtain TIFA protein, pET22b-TIFA vector was transformed into *E. coli* BL21(DE3), or pCS-TIFA-His was transfected into HEK293t cells. TIFA-His was purified using Ni-NTA agarose resin (ThermoFisher).

UV-visible spectroscopy. All UV-visible spectra were recorded on a Nanodrop spectrometer (ThermoFisher) using a 1-cm quartz cuvette at ambient temperature (ca. 25 °C). UV-visible spectra were scanned from 220 to 800 nm. For BCA competition assay, copper (Cu^{1+})-BCA solution was freshly prepared. Aliquots of NTD or NTD-CKD proteins were titrated into Cu^{1+} -BCA solution with gentle mixing, and the UV-visible spectra were recorded after a 10-min incubation. The binding constants between apo-ALPK1 (NTD or NTD-CKD) and Cu^{1+} -BCA ($K_d(\text{Cu-BCA-NTD})$ and $K_d(\text{Cu-BCA-NTD-CKD})$) was determined by fitting UV-vis titration curve to the Ryan-Weber nonlinear equation as described before (3). The average apparent constant of Cu^+ and NTD($K_d'_{\text{Cu-NTD}}$) or NTD-CKD ($K_d'_{\text{Cu-NTD-CKD}}$) was also calculated based on the formation constant (K_a) between Cu^{1+} and BCA is $10^{17.7} \text{ M}^{-2}$ (4).

Mitochondria isolation and ICP-MS. HeLa cells were collected by centrifugation (300 xg, 3 min). After wash, suspension and homogenization steps, mitochondria were isolated using a two-step centrifugation method carried out at low speed (750 x g, 10 min) to remove intact cells, cell debris and nuclei from the whole cell extracts followed by high speed centrifugation (10,000 x g, 15 min) to concentrate mitochondria. Mitochondria samples were subjected to ICP-MS analysis for copper content determination. The standard curve of copper was prepared from multielement standard solution.

Determination of Mitochondria Membrane Potential. Mitochondria membrane potential was determined by JC-1 fluorescent dye (Beyotime) according to the manufacturer's protocol. Briefly, cells were seeded in 12 well plate and were challenged by *Salmonella* with a MOI of 100. At

indicated time points (0, 2, 4, 6, 16 hpi), cells were washed once with PBS and incubated with 0.5 ml of JC-1 staining working solution for 20 min at 37°C. Sequentially, after wash step with JC-1 dye buffer (1X), emission spectra at 405 and 488 nm and excitation spectra at 530 and 595 nm were determined by luminescence spectrometer (Edinburgh Instruments). Mitochondria membrane potential was represented as the ratio of red (595 nm) to green (530 nm) fluorescence intensity.

NF- κ B activation reporter assay. Plasmid pNifty2-SEAP (InvivoGen) was transfected into HeLa or HEK293t cells with Lipo8000™ Transfection Reagent (Beyotime). Cells were treated with copper or ADP-heptose as indicated for 24 hrs. Aliquots of media were transferred to 96-well plate with assay buffer, the SEAP activities in which were determined according to the manufacturer's protocol (InvivoGen) by the read absorbance at 620 nm.

RNA extraction and RT-qPCR. RNAs were extracted using GeneJET RNA Purification Kit (ThermoFisher). qRT-PCR was performed with HiScript II One Step qRT-PCR SYBR Green Kit (Vazyme) according to the manufacture's instruction. $\Delta\Delta$ CT method was applied to quantify the transcription level of target genes by normalizing to the house-keeping gene GAPDH.

Native polyacrylamide gel electrophoresis (PAGE) Assay. Native PAGE (10%) was used to analyze the oligomerization of TIFA with or without copper/ADP-heptose treatment. The native PAGE was prepared without any SDS content. Recombination full-length ALPK1 (200 ng/reaction) and TIFA-His (2 μ g/reaction) proteins were incubated with copper or ADP-heptose as indicated in the presence of 5 mM GSH. ATP (100 μ M final concentration) was added to initial the reaction. After kinase reaction, protein samples were mixed with 4x native PAGE loading buffer (1.0 M Tris-HCl, 1% bromophenol blue and 50% glycerol). The electrophoresis was carried out at 130V for 1 hr on ice with 25 mM Tris-HCl, 250 mM Glycine as running buffer. TIFA was detected by the downstream Western Blot analysis using anti-His antibody (Abmart).

CRISPR-Cas9. Knockout AGS/HeLa cell line was generated using the CRISPR-Cas9 method as described by the Zhang laboratory (5) and primer sequences for gRNAs are listed as below.

Primer name	Sequences
TIFA-sgRNA-top	CACCGATCGTGGACAGCAGAGAGC
TIFA-sgRNA-bottom	AAACGCTCTCTGCTGTCCACGATC
ALPK1-sgRNA-top	CACCGAGAGGACAAAACAAACCTGA
ALPK1-sgRNA-bottom	AAACTCAGGTTTGTTCCTCTG
TLR4-sgRNA-top	CACCGATGATGTCTGCCTCGCGCC
TLR4-sgRNA-bottom	AAACGGCGCGAGGCAGACATCATC
CTR1-sgRNA-top	CACCGCATATAGCTCATCCCCATA
CTR1-sgRNA-bottom	AAACTATGGGGATGAGCTATATGC
SLC25A3-sgRNA-top	CACCGCTGGTGCACGATGGTCTCGGGG
SLC25A3-sgRNA-bottom	AAACCCCGAGACCATCGTGCACCAGC

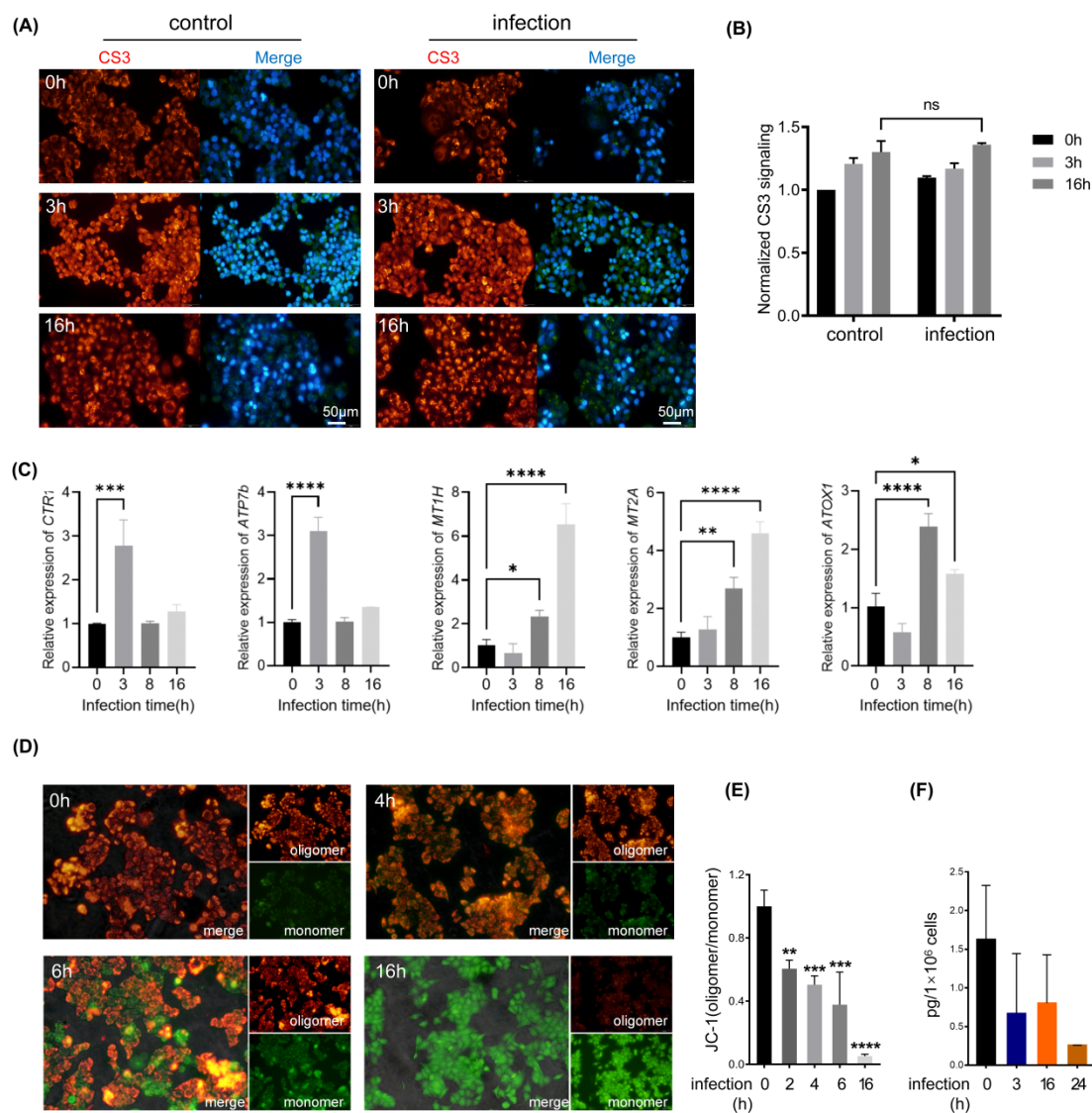


Fig. S1. Host cells actively accumulate copper in cytosol in response to bacterial infection. Related to Fig. 1.

(A) Fluorescence imaging of cytosol Cu in HeLa cells with CS3 staining. HeLa cells incubated with copper (just prior to the infection) were stained with 2 μM CS3 for 10 min at 37 °C in DMEM with/without 3 or 16 hrs *Salmonella* infection. Additional copper (40 μM) in culture medium elevated Cu levels with/without infection.

(B) Graph showing the quantification of mean fluorescence intensity of each condition in (A) (n=3 fields of cells per condition).

(C) Expression levels of transporters and chaperones involving cytosolic Cu homeostasis by RT-qPCR. HeLa cells were infected with *Salmonella* at MOI of 100 and mRNA levels of hCTR1, ATP7b, MT1H, MT2A and ATOX1 were determined by RT-qPCR. The variation in time resolution among different genes implies the intricate regulation of copper homeostasis within host cells.

(D) Fluorescence imaging of HeLa cells with JC-1 staining. HeLa cells were infected with *Salmonella* at MOI of 100 and were stained with JC-1 at time point as indicated (0, 2, 4, 6, 16 hrs).

(E) Graph showing the quantification of mean JC-1 fluorescence intensity of each condition in (A) (n=3 fields of cells per condition).

(F) Cu concentrations in mitochondria measured by ICP-MS. HeLa cells were infected with *Salmonella* at MOI of 100 for 24 hrs. At the indicated time points, mitochondria were separated and subjected to ICP-MS for determination of copper content. Data are shown as mean \pm SEM (n \geq 3). ns, not significant, $p > 0.05$; * $p < 0.05$; ** $p < 0.01$; *** $p < 0.001$; **** $p < 0.0001$.

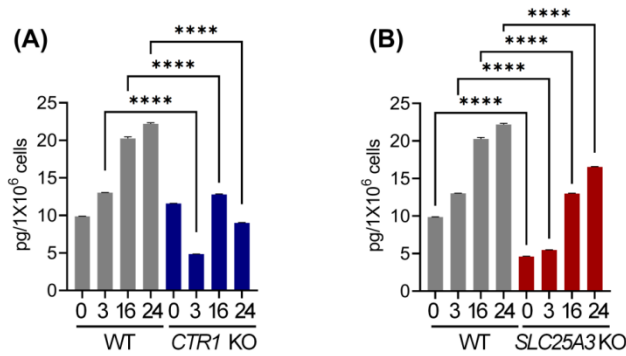


Fig. S2. Total Cu concentrations in cell measured by ICP-MS. HeLa cells (WT, *CTR1* KO, or *SLC25A3* KO) were infected with *Salmonella*, cells were harvested and subjected to ICP-MS for determination of copper content. Data are shown as mean \pm SEM (n \geq 3). ns, not significant, $p > 0.05$; * $p < 0.05$; ** $p < 0.01$; *** $p < 0.001$; **** $p < 0.0001$.

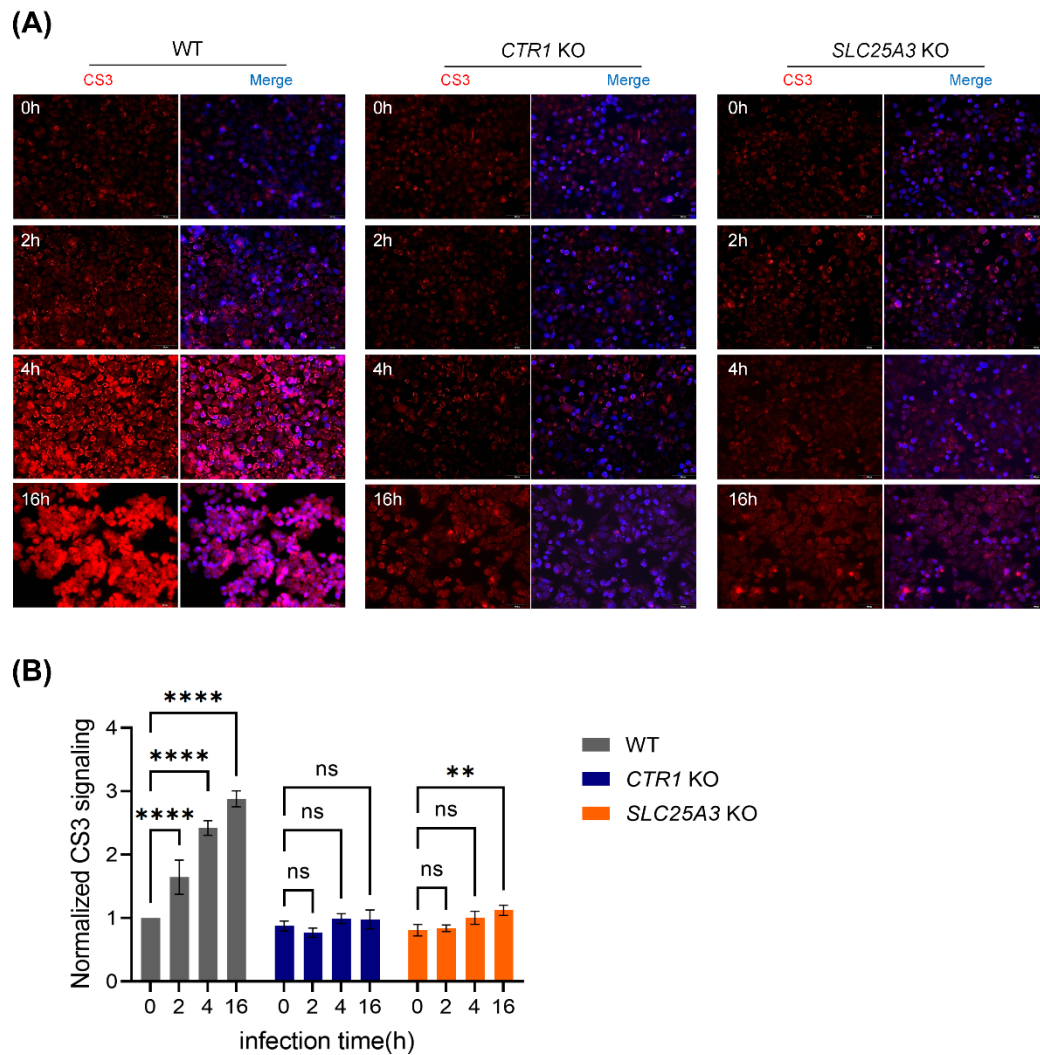
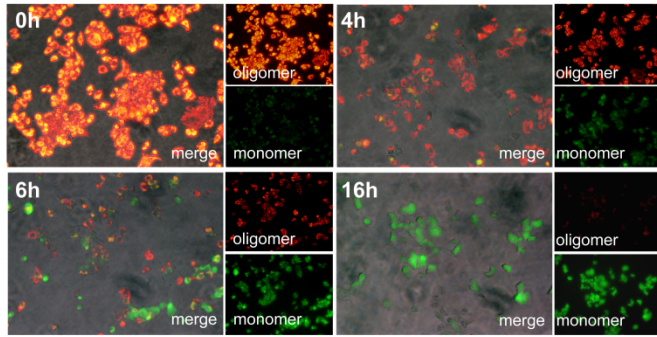
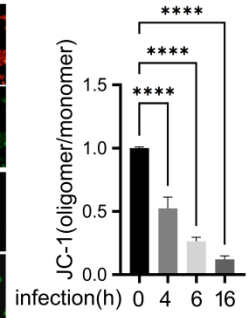


Fig. S3. Copper accumulation in cytosol depends on copper transporter CTR1 and SLC25A3. Related to Fig. 1. (A) Fluorescence imaging of cytosol Cu in CTR1- or SLC25A3-deficient HeLa cells with CS3 staining. (B) Graph showing the quantification of mean fluorescence intensity of each condition in (A) (n=3 fields of cells per condition).

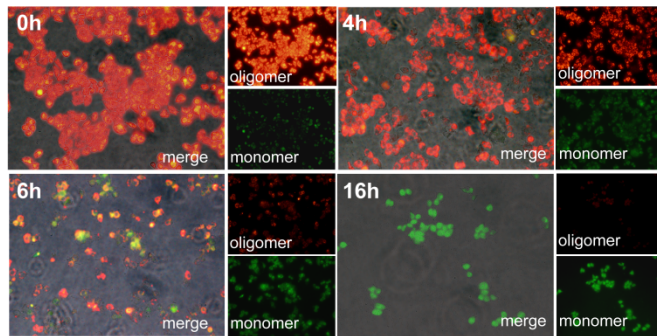
(A) *Salmonella* Typhimurium



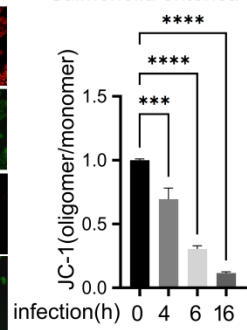
Salmonella Typhimurium



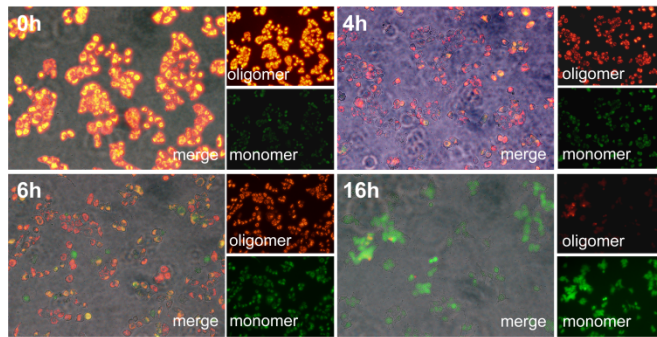
(B) *Salmonella enterica* O2



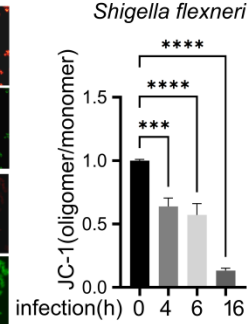
Salmonella enterica O2



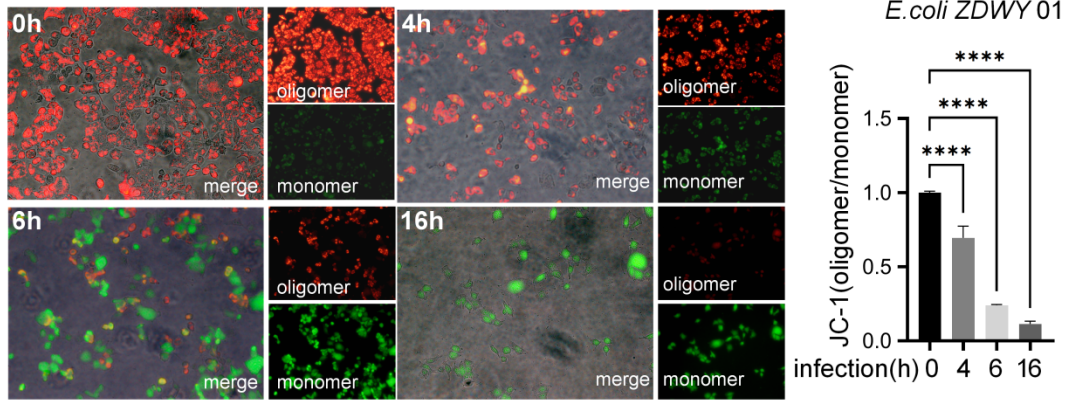
(C) *Shigella flexneri*



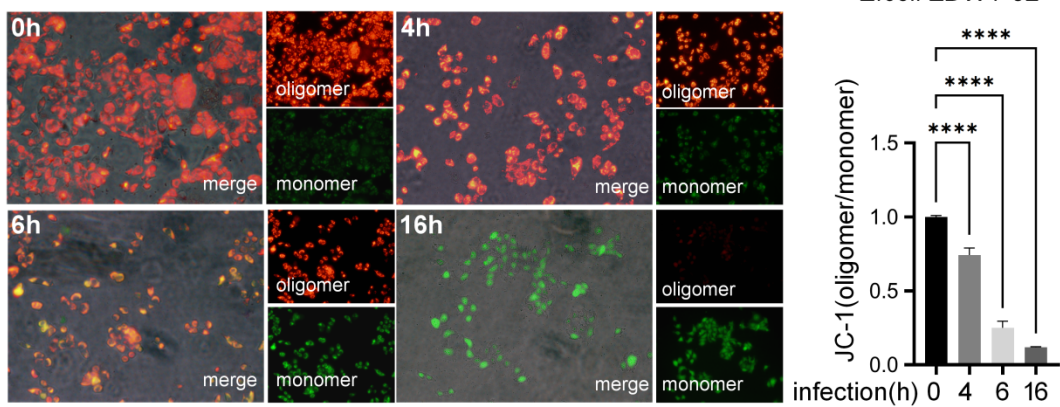
Shigella flexneri



(D) *E. coli* ZDWY 01



(E) *E. coli* ZDWY 02



(F) *Vibrio vulnificus*

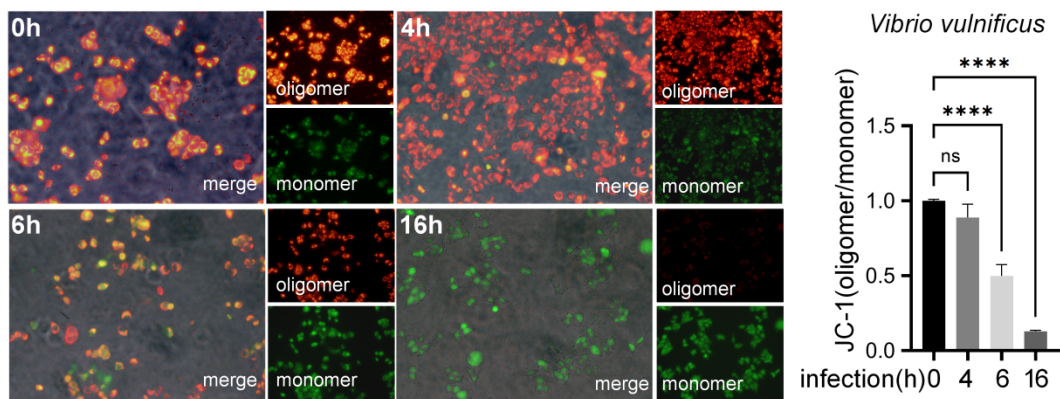


Fig. S4 Effect of bacterial infection on the mitochondrial membrane potential of HeLa cells. HeLa cells were infected with different bacterial pathogens and were stained with JC-1 at time point as indicated (0, 4, 6, 16 hrs).

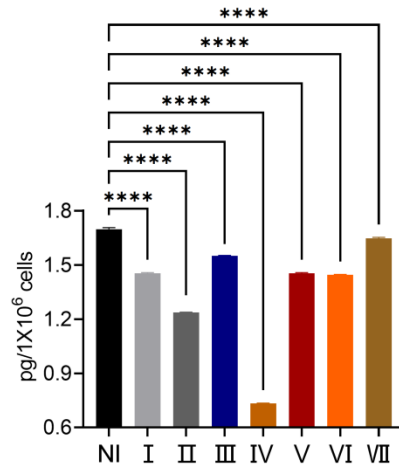


Fig. S5. Cu concentrations in mitochondria measured by ICP-MS. Related to Fig. 1. HeLa cells were infected with bacterial pathogens for 24 hrs. Mitochondria were separated and subjected to ICP-MS for determination of copper content. NI:non-infection, I:*Salmonella enterica* 01, II:*Salmonella* Typhimurium, III:*Salmonella enterica* 02, IV:*Shigella flexneri*, V:*E.coli* ZDWY 01 VI:*E.coli* ZDWY 02, VII:*Vibrio vulnificus*. Data are shown as mean \pm SEM ($n \geq 3$). ns, not significant, $p > 0.05$; * $p < 0.05$; ** $p < 0.01$; *** $p < 0.001$; **** $p < 0.0001$.

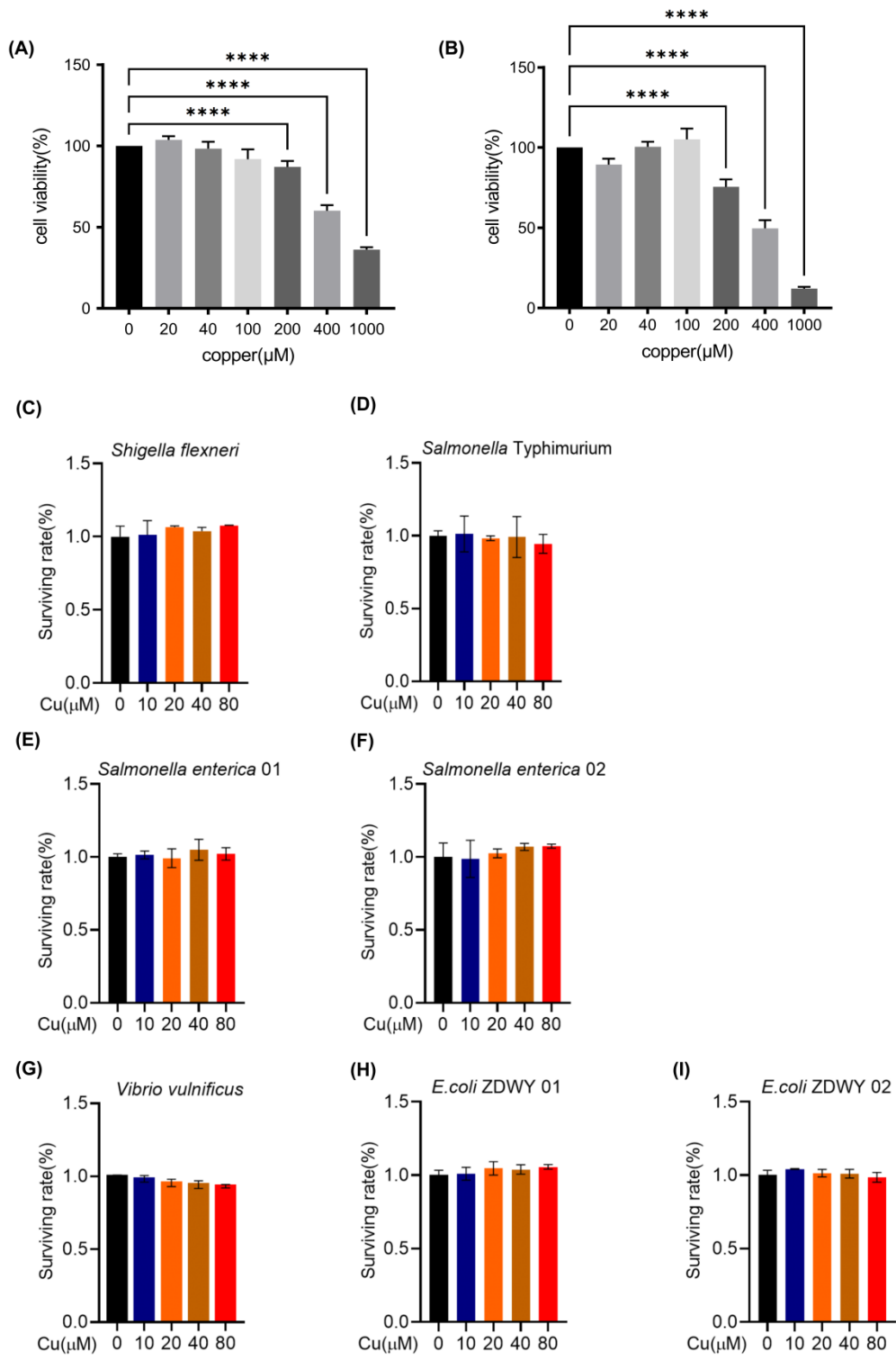


Fig. S6. Effect of Copper treatment on the cell viability of host cells and bacteria. Related to Fig. 1.

(A) Cell viability of HeLa cells with copper treatment (3 hrs) was determined with MTT assay.

(B) Cell viability of HeLa cells with copper treatment (8 hrs) determined with MTT assay. The treatment of copper (0-100 μM) did not result in reduced viability of host cells.

(C-I) Viability of bacterial strains with copper treatment. Data are shown as mean \pm SEM ($n \geq 3$). ns, not significant, $p > 0.05$; * $p < 0.05$; ** $p < 0.01$; *** $p < 0.001$; **** $p < 0.0001$.

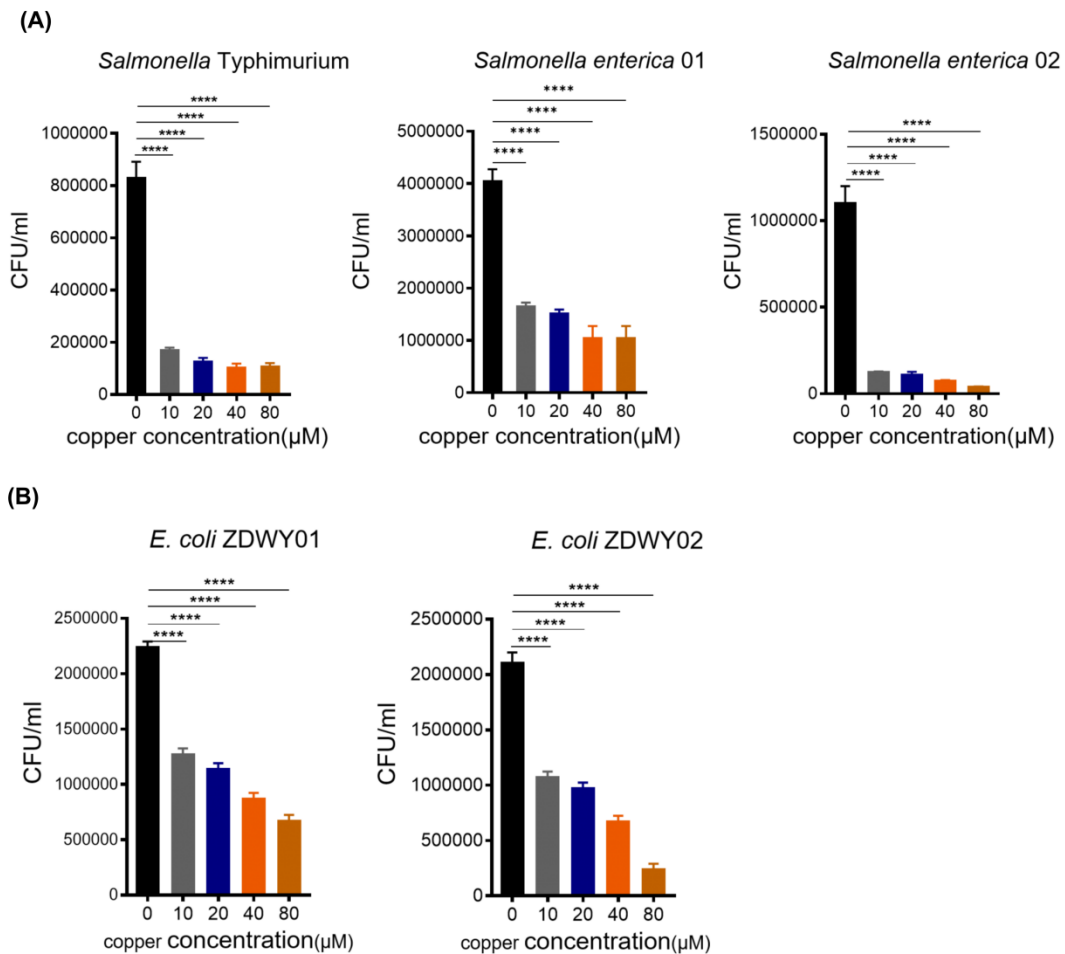


Fig. S7. Assessing Cu effect on host cell defense against bacteria pathogen. Related to Fig. 1.

(A) CFUs of intracellular pathogen *Salmonella Typhimurium* and *Salmonella enterica* strains recovered from HeLa cells in gentamycin protection assay.

(B) CFUs of extracellular pathogen *E. coli* strains in bacterial adhesion assay. Data are shown as mean \pm SEM ($n \geq 3$). ns, not significant, $p > 0.05$; * $p < 0.05$; ** $p < 0.01$; *** $p < 0.001$; **** $p < 0.0001$.

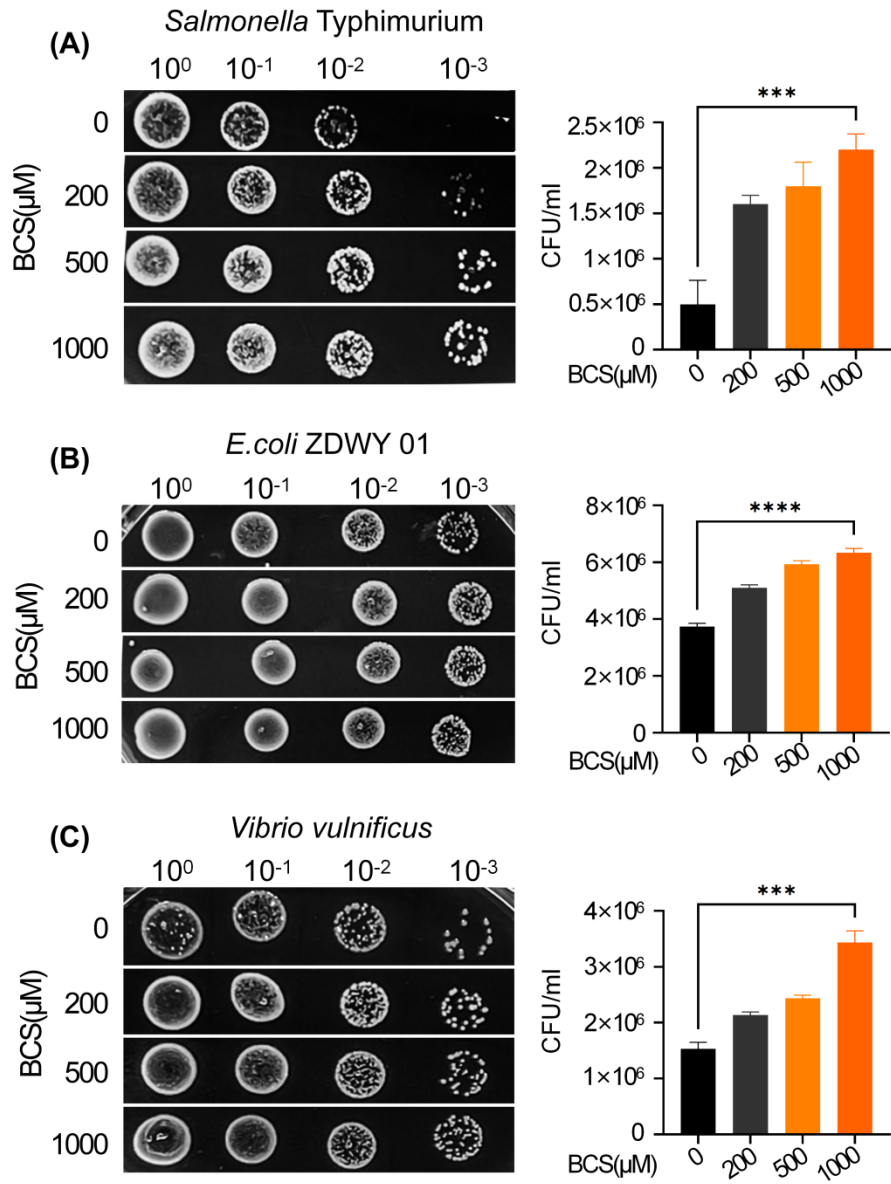


Fig. S8. Assessing effect of Cu chelator BCS on host cell defense against bacteria pathogens. Related to Fig. 1. Data are shown as mean \pm SEM ($n \geq 3$). ns, not significant, $p > 0.05$; * $p < 0.05$; ** $p < 0.01$; *** $p < 0.001$; **** $p < 0.0001$.

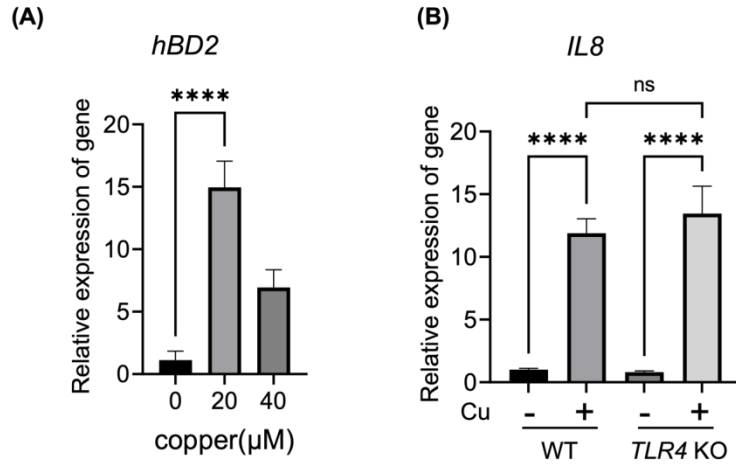


Fig. S9. Quantitative real-time PCR analysis of gene expression in host cells upon Cu treatment. Related to Fig. 2.

(A) hBD2 expression in host cells upon Cu treatment.

(B) IL8 expression in host cells (WT vs *TLR4* KO) upon Cu. Data are shown as mean ± SEM (n≥3). ns, not significant, $p > 0.05$; * $p < 0.05$; ** $p < 0.01$; *** $p < 0.001$; **** $p < 0.0001$.



Fig. S10. Sequence alignment of ALPK1 wild type and KO. Related to Fig. 2. The target site for sgRNA is highlighted.

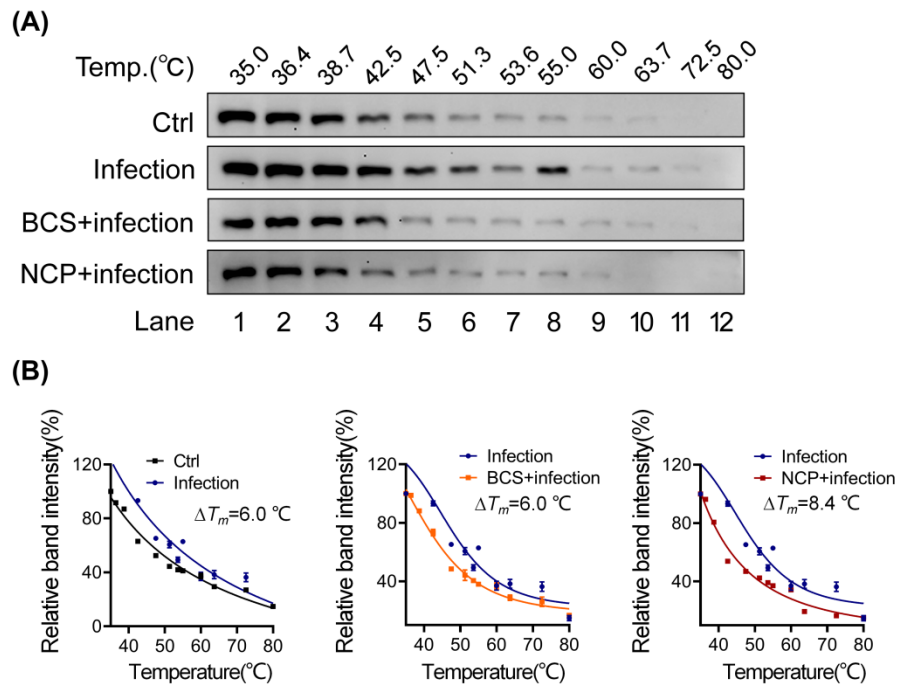


Fig. S11. Effect of infection and copper on the thermal stability of ALPK1. Related to Fig. 3.

(A). Representative CETSA blot for thermal stability of ALPK1 in cell. HEK293t cells expressing ALPK1-flag were pretreated with/without BCS or NCP following bacterial infection. Cells were harvested and treated with the indicated heat shocks. Soluble ALPK1-flag in sample supernatant was revealed by immunoblotting with anti-Flag antibody.

(B). CETSA melt curves for the thermal stability of ALPK1 in cell. The melting temperatures shift (ΔT_m) between treated and control samples was measured.

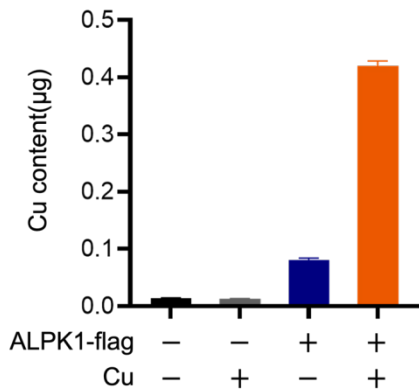


Fig. S12. Determination of Cu content in protein samples extracted from HEK293t cells via ICP-MS. Related to Fig. 3.

HEK293t cells harboring ALPK1-flag expression vector or control cells were pretreated with/without Cu. Flag-fused protein was extracted from HEK293t using anti-Flag magnetic beads. Cu content in protein samples was determined with ICP-MS.

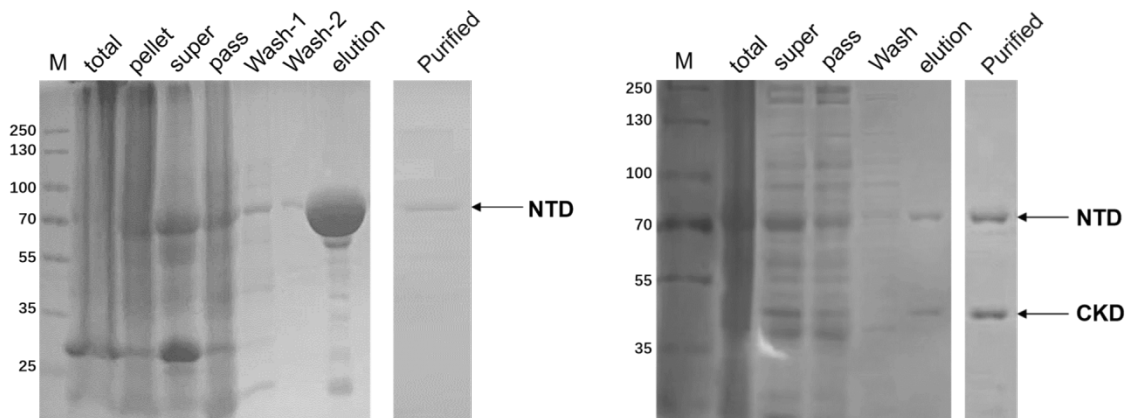


Fig. S13. SDS-PAGE analysis of NTD and NTD-CKD recombination protein purification. Related to Fig. 3.

The gels were stained with Coomassie blue G250. Lanes: M, molecular mass standards (kDa).

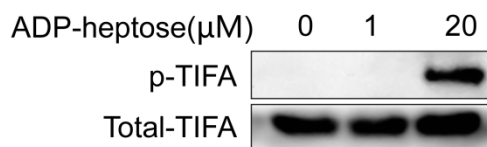


Fig. S14. Representative Western Blot for p-TIFA *in vitro*. Related to Fig. 3. Recombinant ALPK1 and TIFA proteins were incubated with ADP-heptose (1 or 20 µM, 1 hrs), phosphorylated TIFA was revealed by immunoblotting with anti-p-TIFA antibody. Noticeably, the low concentration of ADP-heptose (1 µM), a concentration that is present in bacteria, was not able to induce p-TIFA in this reaction.

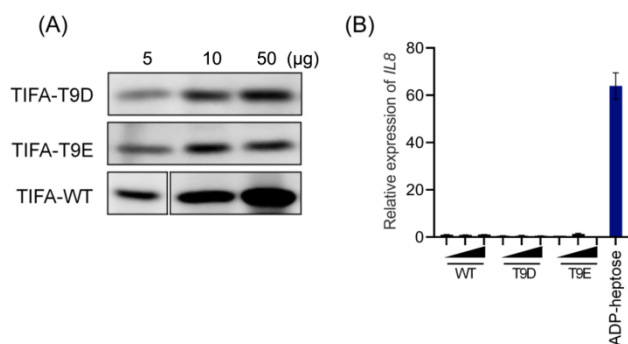


Fig. S15. The phosphor-mimetic of TIFA is not sufficient to activate NF- κ B. Related to Fig. 3. (A) Representative western blot for TIFA in cell. Gradient amounts (5, 10, 50 μ g) of recombinant His tag-labeled TIFA proteins (WT, T9D or T9E) were transfected into HeLa cells, TIFA were revealed by immunoblotting with anti-His. (B) Quantitative real-time PCR analysis of IL8 expression in HeLa cells.

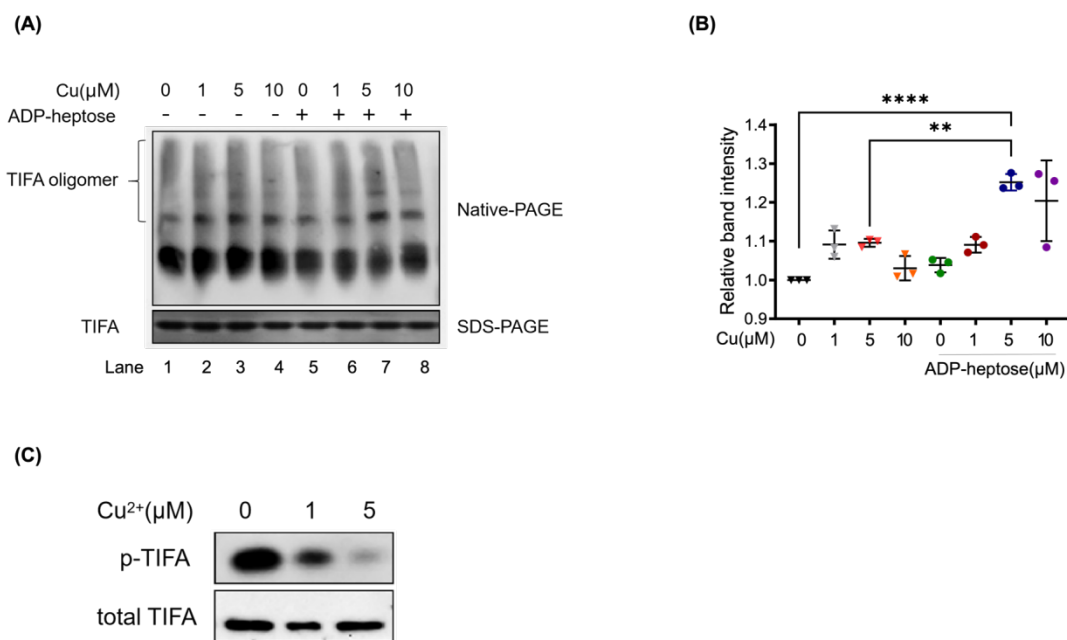


Fig. S16. Effect of copper on ALPK1 kinase activity *in vitro*. Related to Fig. 3.

(A) Representative Western Blot for TIFA oligomerization assay *in vitro* using Native-PAGE. Recombination ALPK1 and TIFA proteins were mixed with indicated concentrations of Cu in the presence of 5mM GSH, with/without ADP-heptose (5 μ M). Copper promotes the ALPK1-mediated formation of TIFA oligomer *in vitro*.

(B) Graph showing the quantification of mean band intensity of each condition in(A). ** $p < 0.01$; **** $p < 0.0001$.

(C) Cu²⁺ suppresses ADP-heptose-induced ALPK1 kinase activity *in vitro* in the absence of GSH. Recombination ALPK1 and TIFA proteins were mixed with indicated concentrations of Cu²⁺ in the presence of ADP-heptose.

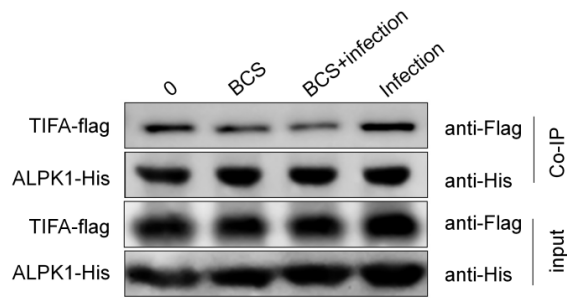


Fig. S17. Interaction between ALPK1 and TIFA during bacterial infection depends on the copper availability. Related to Fig. 3.

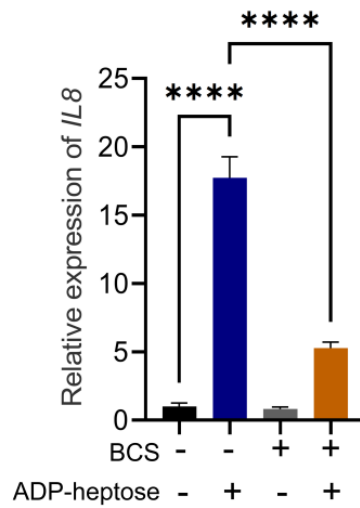


Fig. S18. Quantitative real-time PCR analysis of IL8 expression in HeLa cells upon BCS treatment (500 μ M). Related to Fig. 4. Data are shown as mean \pm SEM ($n \geq 3$). ns, not significant, $p > 0.05$; * $p < 0.05$; ** $p < 0.01$; *** $p < 0.001$; **** $p < 0.0001$.

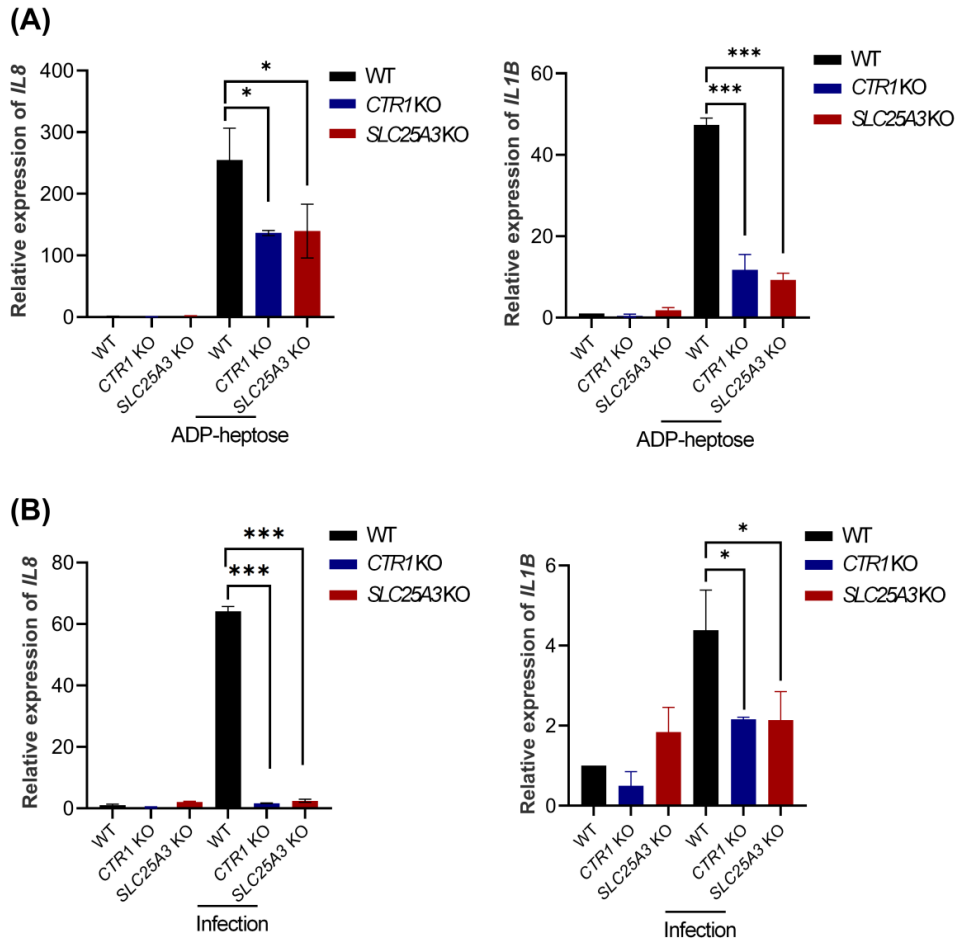
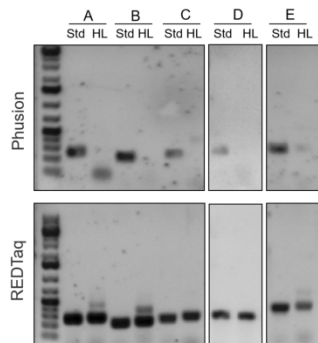
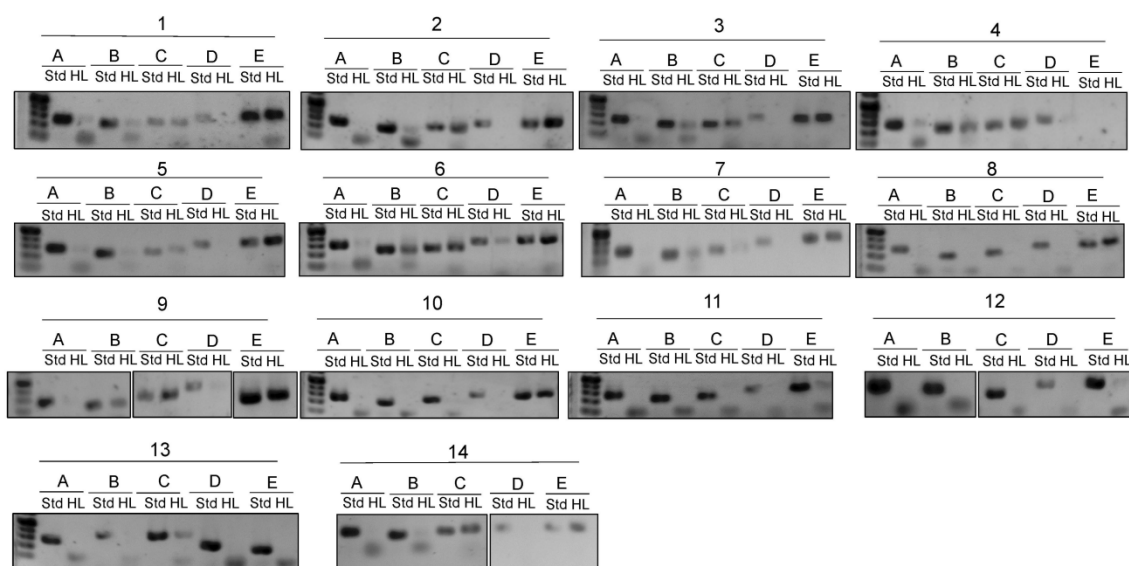


Fig. S19. The *CTR1*- or *SLC25A3* deficiency attenuates host cell response to ADP-heptose stimulation and bacterial infection. Related to Fig. 4.
 (A) Quantitative real-time PCR analysis of *IL8* and *IL1B* expression in HeLa cells upon ADP-heptose stimulation.
 (B) Quantitative real-time PCR analysis of *IL8* and *IL1B* expression in HeLa cells upon bacterial infection.

(A) *alpk1*(uninjected)



(B) *alpk1*(injected)



(C)

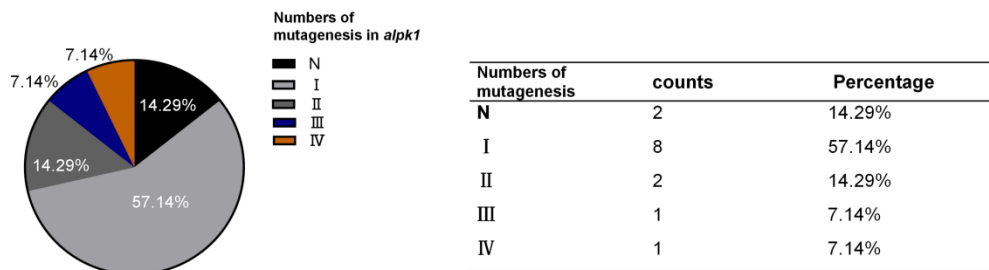


Fig. S20. CRISPR-Cas9 method to establish F0 *alpk1* knockout fish. Related to Fig. 4.

alpk1 gene was targeted at 5 loci with 5 gRNAs (gRNA A-E) simultaneously. Headloop PCR is used to validate *alpk1* knockout in zebrafish. No amplification with headloop primers is detected for the loci without mutagenesis; in contrast, amplification of the targeted loci indicates there is mutagenesis in the loci. The headloop score (HL score) for *alpk1* was calculated as the ratio

between the headloop PCR band intensity (HL) and the standard PCR band intensity (std). At least one gRNA has a high headloop PCR score (>0.6) in most tested fish embryos confirm that mutagenesis is high in *alpk1* gene (except 11 and 12).

References

1. F. Kroll *et al.*, A simple and effective F0 knockout method for rapid screening of behaviour and other complex phenotypes. *eLife* **10**, e59683 (2021).
2. P. Zhou *et al.*, Alpha-kinase 1 is a cytosolic innate immune receptor for bacterial ADP-heptose. *Nature* **561**, 122-126 (2018).
3. X. Yang, H. Li, T. P. Lai, H. Sun, UreE-UreG complex facilitates nickel transfer and preactivates GTPase of UreG in *Helicobacter pylori*. *J Biol Chem* **290**, 12474-12485 (2015).
4. P. Bagchi, M. T. Morgan, J. Bacsá, C. J. Fahrni, Robust affinity standards for Cu(I) biochemistry. *J Am Chem Soc* **135**, 18549-18559 (2013).
5. F. A. Ran *et al.*, Genome engineering using the CRISPR-Cas9 system. *Nat Protoc* **8**, 2281-2308 (2013).